Inorg. Chem. **2005**, *44*, 5719–5727

Diosmium(III) Compounds Supported by 2-Anilinopyridinate and Novel Alkynyl Derivatives

Yan-Hui Shi,[†] Wei-Zhong Chen,[†] Kevin D. John,[‡] Ryan E. Da Re,[‡] Joshua L. Cohn,[§] Guo-Lin Xu,[†] Judith L. Eglin,[‡] Alfred P. Sattelberger,[‡] Curtis R. Hare,[†] and Tong Ren*[,†]

Department of Chemistry, University of Miami, Coral Gables, Florida 33146, Los Alamos National Laboratory, Los Alamos, New Mexico 87545, and Department of Physics, University of Miami, Coral Gables, Florida 33124

Received April 4, 2005

The reaction between $Os_2(OAc)_4Cl_2$ and H*ap* (H*ap* is 2-anilinopyridine) under prolonged refluxing conditions resulted in an Os^{III}_2 compound, $Os_2(ap)_4Cl_2$ (**1**), that can be crystallized as either the *cis*-(2,2) isomer from a CH_3OH–CH_2Cl_2 solution or the (3,1) isomer from a hexanes–CH_2Cl_2 solution. Compound **1** undergoes facile reactions with LiC_2Y to yield a series of $Os_2(ap)_4(C_2Y)_2$ compounds with Y as Ph (**2**), ferrocenyl (**3**), $SiMe_3$ (**4**), and C_2SiMe_3 (**5**). X-ray diffraction study of compound **2** reveals solvent-dependent isomerism similar to that of the parent compound **1**. Compound **1** has Os–Os distances of 2.3937(8) and 2.3913(8) Å for the *cis*-(2,2) and (3,1) isomers, respectively, and is paramagnetic ($S = 1$). Both the ethynyl derivatives **2**–**4** and butadiynyl derivative **5** are diamagnetic and have Os–Os distances of 2.456(1), 2.471(1), and 2.481(1) Å for the *cis*-(2,2) and (3,1) isomers of **2** and (3,1) isomer of **4**, respectively. Compounds **1**–**5** exhibit multiple one-electron redox couples in their cyclic voltammograms, including a reversible Os_2(8+/7+) couple for **2**. Resonance Raman spectra of both compounds **1** and **2** are reported.

Introduction

The chemistry of dinuclear species containing metal−metal multiple bonds has been traditionally dominated by compounds based on both the group 6 elements and Re.[1] Recent decades have witnessed a rapid expansion in diruthenium chemistry because of contributions from the laboratories of Cotton,[2] Bear and Kadish,[3] Dunbar,[4] Jiménez-Aparicio,[5] Kitagawa,[6] Ren,[7−9] and others.[10] Diosmium chemistry, on the other hand, has received very limited attention.[11] Recent isolation and structural characterization of $[Os_2(hpp)_4Cl_2]^+$ (*hpp* is 1,3,4,6,7,8-hexahydro-*2H*-pyrimido[1,2-*a*]pyrimidinate), the first ever $M^{III}M^{IV}$ paddlewheel species, highlights the significance of diosmium compounds in the understanding of multiple bonds between metal atoms.[12] The presence of axial halide ligands has been a fixture of Os^{III}_2 paddlewheel species, and it is of interest whether these halides can be exchanged with acetylides in analogy to the alkynylation reaction for diruthenium species.[7] In addition to $Os_2(hpp)_4Cl_2$, $Os_2(DtolF)_4Cl_2$ (*D*tol*F* is di(*p*-tolyl)formamidinate) is the other diosmium paddlewheel compound supported by

* Author to whom correspondence should be addressed. E-mail: tren@miami.edu. Tel.: (305) 284-6617. Fax: (305) 284-1880.
[†] Department of Chemistry, University of Miami.
[‡] Los Alamos National Laboratory.
[§] Department of Physics, University of Miami.

(1) Cotton, F. A.; Walton, R. A. *Multiple Bonds between Metal Atoms*; Oxford University Press: Oxford, U.K., 1993.

(2) (a) Angaridis, P.; Cotton, F. A.; Murillo, C. A.; Villagrán, D.; Wang, X. *J. Am. Chem. Soc.* **2005**, *127*, 5008. (b) Angaridis, P.; Cotton, F. A.; Murillo, C. A.; Villagrán, D.; Wang, X. *Inorg. Chem.* **2004**, *43*, 8290. (c) Cotton, F. A.; Murillo, C. A.; Reibenspies, J. H.; Villagrán, D.; Wang, X.; Wilkinson, C. C. *Inorg. Chem.* **2004**, *43*, 8373. (d) Angaridis, P.; Berry, J. F.; Cotton, F. A.; Murillo, C. A.; Wang, X. *J. Am. Chem. Soc.* **2003**, *125*, 10327. (e) Angaridis, P.; Berry, J. F.; Cotton, F. A.; Lei, P.; Lin, C.; Murillo, C. A.; Villagrán, D. *Inorg. Chem. Commun.* **2004**, *7*, 9. (f) Cotton, F. A.; Stiriba, S. E.; Yokochi, A. *J. Organomet. Chem.* **2000**, *595*, 300. (g) Cotton, F. A.; Yokochi, A. *Inorg. Chem.* **1997**, *36*, 567. (h) Cotton, F. A.; Lu, J.; Yokochi, A. *Inorg. Chim. Acta* **1998**, *276*, 447. (i) Cotton, F. A.; Yokochi, A. *Polyhedron* **1998**, *17*, 959. (j) Cotton, F. A.; Yokochi, A. *Inorg. Chim. Acta* **1998**, *276*, 557. (k) Cotton, F. A.; Yokochi, A. *Inorg. Chem.* **1998**, *37*, 2723. (l) Cotton, F. A.; Kim, Y. M.; Yokochi, A. *Inorg. Chim. Acta* **1995**, *236*, 55.

(3) (a) Kadish, K. M.; Phan, T. D.; Giribabu, L.; Shao, J.; Wang, L.-L.; Thuriere, A.; Caemelbecke, E. V.; Bear, J. L. *Inorg. Chem.* **2004**, *43*, 1012. (b) Kadish, K. M.; Wang, L.-L.; Thuriere, A.; Caemelbecke, E. V.; Bear, J. L. *Inorg. Chem.* **2003**, *42*, 834. (c) Kadish, K. M.; Wang, L.-L.; Thuriere, A.; Giribabu, L.; Garcia, R.; Caemelbecke, E. V.; Bear, J. L. *Inorg. Chem.* **2003**, *42*, 8309. (d) Bear, J. L.; Chen, W.-Z.; Han, B.; Huang, S.; Wang, L.-L.; Thuriere, A.; Caemelbecke, E. V.; Kadish, K. M.; Ren, T. *Inorg. Chem.* **2003**, 6230. (e) Bear, J. L.; Li, Y.; Han, B.; Caemelbecke, E. V.; Kadish, K. M. *Inorg. Chem.* **1996**, *35*, 3053. (f) Bear, J. L.; Han, B.; Huang, S.; Kadish, K. M. *Inorg. Chem.* **1996**, *35*, 3012.

10.1021/ic050496r CCC: $30.25
Published on Web 07/07/2005

N,N′-bidentate bridging ligand.[13] Early study of the reaction between $Os_2(OAc)_4Cl_2$ and H*ap* (2-anilinopyridine) in the presence of Me_3SiCl resulted in an unusual compound $Os_2(ap)_3Cl_3$.[14] We reported recently that the prolonged reflux of $Os_2(OAc)_4Cl_2$ with H*ap* yielded paramagnetic $Os_2(ap)_4Cl_2$ (**1**), which was structurally characterized as a *cis*-(2,2) compound.[15] Described herein are the synthesis, electrochemical, and spectroscopic characterization of a series of bis(alkynyl) derivatives $Os_2(ap)_4(C_2Y)_2$ with Y as Ph (**2**), Fc (**3**), $SiMe_3$ (**4**), and C_2SiMe_3 (**5**) and a solvent-dependent regioisomerism observed for compounds **1** and **2**.

Results and Discussion

Synthesis and Structural Characterization of $Os_2(ap)_4Cl_2$ (1). Preparation of compound **1** is the same as previously reported:[15] refluxing $Os_2(OAc)_4Cl_2$ with 8 equiv of H*ap* resulted in $Os_2(ap)_4Cl_2$ as dark blue crystalline material in satisfactory yield. To authenticate the newly prepared material, a crystal grown under the same conditions as previously reported (CH_3OH/CH_2Cl_2)[15] was examined and yielded an orthorhombic cell instead of the original triclinic cell. The subsequent structural solution revealed that the compound that crystallized, shown in Figure 1, is the previously reported *cis*-(2,2)-$Os_2(ap)_4Cl_2$ (**1a**). We were surprised, however, that materials from the same reaction afforded crystals of a different unit cell when crystallized from hexanes/CH_2Cl_2, and crystallographic analysis revealed a regioisomer of **1a**: (3,1)-$Os_2(ap)_4Cl_2$ (**1b**, Figure 2). In an attempt to eliminate the possibility of the separation of isomers upon crystallization, five randomly picked crystals from each batch were indexed and yielded the identical cell parameters within each batch. However, mixed results were obtained on examining the bulk materials by X-ray powder diffraction (XPD): the bulk sample prepared from CH_3OH/CH_2Cl_2 diffusion (conditions for **1a**) yielded a pattern that agrees with the one calculated from the single-crystal

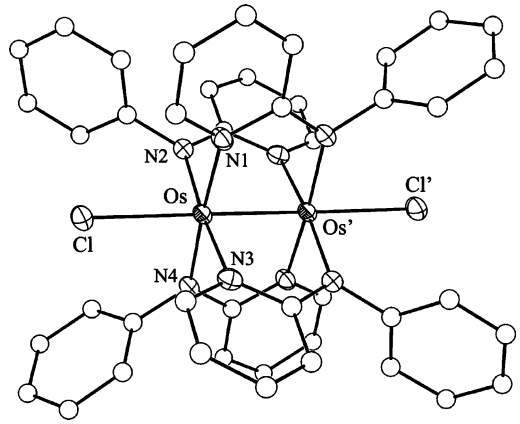

Figure 1. ORTEP plot of molecule **1a** at 30% probability level. Hydrogen atoms were omitted for clarity.

(4) (a) Campos-Fernández, C. S.; Thomson, L. M.; Galán-Mascarós, J. R.; Xiang, O. Y.; Dunbar, K. R. *Inorg. Chem.* **2002**, *41*, 1523. (b) Miyasaka, H.; Clerac, R.; Campos-Fernández, C. S.; Dunbar, K. R. *J. Chem. Soc., Dalton Trans.* **2001**, 858. (c) Miyasaka, H.; Clérac, R.; Campos-Fernández, C. S.; Dunbar, K. R. *Inorg. Chem.* **2001**, *40*, 1663. (d) Miyasaka, H.; Campos-Fernández, C. S.; Clérac, R.; Dunbar, K. R. *Angew. Chem., Int. Ed.* **2000**, *39*, 3831. (e) Campos-Fernández, C. S.; Xiang, O. Y.; Dunbar, K. R. *Inorg. Chem.* **2000**, *39*, 2432.

(5) (a) Barral, M. C.; Herrero, S.; Jiménez-Aparicio, R.; Torres, M. R.; Urbanos, F. A. *Angew. Chem., Int. Ed.* **2004**, *44*, 305. (b) Barral, M. C.; Herrero, S.; Jiménez-Aparicio, R.; Torres, M. R.; Urbanos, F. A. *Inorg. Chem. Commun.* **2004**, *7*, 42. (c) Barral, M. C.; Gonzalez-Prieto, R.; Jiménez-Aparicio, R.; Priego, J. L.; Torres, M. R.; Urbanos, F. A. *Eur. J. Inorg. Chem.* **2003**, 2339. (d) Jiménez-Aparicio, R.; Urbanos, F. A.; Arrieta, J. M. *Inorg. Chem.* **2001**, *40*, 613. (e) Barral, M. C.; Jiménez-Aparicio, R.; Pérez-Quintanilla, D.; Priego, J. L.; Royer, E. C.; Torres, M. R.; Urbanos, F. A. *Inorg. Chem.* **2000**, *39*, 65. (f) Barral, M. C.; Jiménez-Aparicio, R.; Priego, J. L.; Royer, E. C.; Urbanos, F. A.; Amador, U. *Inorg. Chem.* **1998**, *37*, 1413.

(6) (a) Kondo, M.; Hamatani, M.; Kitagawa, S.; Pierpont, C. G.; Unoura, K. *J. Am. Chem. Soc.* **1998**, *120*, 455. (b) Miyasaka, H.; Chang, H.-C.; Mochizuki, K.; Kitagawa, S. *Inorg. Chem.* **2001**, *40*, 3544. (c) Furukawa, S.; Kitagawa, S. *Inorg. Chem.* **2004**, *43*, 6464. (d) Furukawa, S.; Ohba, M.; Kitagawa, S. *Chem. Commun.* **2005**, 865.

(7) (a) Ren, T.; Xu, G.-L. *Comments Inorg. Chem.* **2002**, *23*, 355. (b) Hurst, S. K.; Ren, T. *J. Organomet. Chem.* **2003**, *670*, 188. (c) Ren, T. *Coord. Chem. Rev.* **1998**, *175*, 43.

(8) (a) Shi, Y.; Yee, G. T.; Wang, G.; Ren, T. *J. Am. Chem. Soc.* **2004**, *126*, 10552. (b) Xu, G.-L.; Zou, G.; Ni, Y.-H.; DeRosa, M. C.; Crutchley, R. J.; Ren, T. *J. Am. Chem. Soc.* **2003**, *125*, 10057. (c) Ren, T. *Organometallics* **2002**, *21*, 732. (d) Hurst, S. K.; Ren, T. *J. Organomet. Chem.* **2002**, *660*, 1. (e) Xu, G.-L.; Ren, T. *J. Organomet. Chem.* **2002**, *655*, 239. (f) Xu, G.-L.; Ren, T. *Organometallics* **2001**, *20*, 2400. (g) Zou, G.; Alvarez, J. C.; Ren, T. *J. Organomet. Chem.* **2000**, *596*, 152. (h) Ren, T.; Zou, G.; Alvarez, J. C. *Chem. Commun.* **2000**, 1197.

(9) (a) Xu, G.-L.; DeRosa, M. C.; Crutchley, R. J.; Ren, T. *J. Am. Chem. Soc.* **2004**, *126*, 3728. (b) Xu, G.-L.; Jablonski, C. G.; Ren, T. *J. Organomet. Chem.* **2003**, *683*, 388. (c) Hurst, S. K.; Xu, G.-L.; Ren, T. *Organometallics* **2003**, *22*, 4118. (d) Xu, G.-L.; Jablonski, C. G.; Ren, T. *Inorg. Chim. Acta* **2003**, *343*, 387. (e) Xu, G.-L.; Campana, C.; Ren, T. *Inorg. Chem.* **2002**, *41*, 3521. (f) Chen, W.-Z.; Ren, T. *Inorg. Chem.* **2003**, *42*, 8847. (g) Ren, T.; DeSilva, V.; Zou, G.; Lin, C.; Daniels, L. M.; Campana, C. F.; Alvarez, J. C. *Inorg. Chem. Commun.* **1999**, *2*, 301. (h) Lin, C.; Ren, T.; Valente, E. J.; Zubkowski, J. D. *J. Organomet. Chem.* **1999**, *579*, 114. (i) Lin, C.; Ren, T.; Valente, E. J.; Zubkowski, J. D. *J. Chem. Soc., Dalton Trans.* **1998**, 571. (j) Lin, C.; Ren, T.; Valente, E. J.; Zubkowski, J. D.; Smith, E. T. *Chem. Lett.* **1997**, 753. (k) Xu, G.-L.; Cordova, A.; Ren, T. *J. Cluster Sci.* **2004**, *15*, 413. (l) Chen, W.-Z.; Ren, T. *Organometallics* **2004**, *23*, 3766. (m) Chen, W.-Z.; Ren, T. *Organometallics* **2005**, *24*, 2660.

(10) (a) Liao, Y.; Shum, W. W.; Miller, J. S. *J. Am. Chem. Soc.* **2002**, *124*, 9336. (b) Vos, T. E.; Liao, Y.; Shum, W. W.; Her, J.-H.; Stephens, P. W.; Reiff, W. M.; Miller, J. S. *J. Am. Chem. Soc.* **2004**, *126*, 11630. (c) Miyasaka, H.; Sugiura, K.; Yamashita, M. *Inorg. Chem. Commun.* **2003**, *6*, 1078. (d) Miyasaka, H.; Izawa, T.; Sugiura, K.; Yamashita, M. *Inorg. Chem.* **2003**, *42*, 7683. (e) Aquino, M. A. S. *Coord. Chem. Rev.* **2004**, *248*, 1025. (f) Briand, G. G.; Cooke, M. W.; Cameron, T. S.; Farrell, H. M.; Burchell, T. J.; Aquino, M. A. S. *Inorg. Chem.* **2001**, *40*, 3267. (g) Cooke, M. W.; Cameron, T. S.; Robertson, K. N.; Swarts, J. C.; Aquino, M. A. S. *Organometallics* **2002**, *21*, 5962. (h) Chisholm, M. H.; Christou, G.; Folting, K.; Huffman, J. C.; James, C. A.; Samuels, J. A.; Wesemann, J. L.; Woodruff, W. H. *Inorg. Chem.* **1996**, *35*, 3643. (i) Wesemann, J. L.; Chisholm, M. H. *Inorg. Chem.* **1997**, *36*, 3258. (j) Miyasaka, H.; Kachi-Terajima, C.; Ishii, T.; Yamashita, M. *J. Chem. Soc., Dalton Trans.* **2001**, 1929. (k) Yoshioka, D.; Mikuriya, M.; Handa, M. *Chem. Lett.* **2002**, 1044. (l) Sayama, Y.; Handa, M.; Mikuriya, M.; Hiromitsu, I.; Kasuga, K. *Bull. Chem. Soc. Jpn.* **2003**, *75*, 769. (m) Sayama, Y.; Handa, M.; Mikuriya, M.; Hiromitsu, I.; Kasuga, K. *Chem. Lett.* **1999**, 453. (n) Handa, M.; Yoshioka, D.; Sayama, Y.; Shiomi, K.; Mikuriya, M.; Hiromitsu, I.; Kasuga, K. *Chem. Lett.* **1999**, 1033. (o) Zuo, J.-L.; Herdtweck, E.; Kühn, F. E. *J. Chem. Soc., Dalton Trans.* **2002**, 1244.

(11) Ren, T. In *Multiple Bonds between Metal Atoms*, 3rd ed.; Cotton, F. A., Walton, R. A., Murillo, C. A., Eds.; Springer Science and Business Media, Inc.: New York, 2005.

(12) (a) Cotton, F. A.; Dalal, N. S.; Huang, P.; Murillo, C. A.; Stowe, A. C.; Wang, X. *Inorg. Chem.* **2003**, *42*, 670. (b) Clérac, R.; Cotton, F. A.; Daniels, L. M.; Donahue, J. P.; Murillo, C. A.; Timmons, D. J. *Inorg. Chem.* **2000**, *39*, 2581.

(13) Cotton, F. A.; Ren, T.; Eglin, J. L. *Inorg. Chem.* **1991**, *30*, 2559.

(14) Chakravarty, A. R.; Cotton, F. A.; Tocher, D. A. *Inorg. Chem.* **1984**, *23*, 4693.

(15) Ren, T.; Parrish, D. A.; Deschamps, J. R.; Eglin, J. L.; Xu, G.-L.; Chen, W.-Z.; Moore, M. H.; Schull, T. L.; Pollack, S. K.; Shashidhar, R.; Sattelberger, A. P. *Inorg. Chim. Acta* **2004**, *357*, 1313.

Chart 1. Possible Ligand Arrangements in an $M_2(ap)_4$ Compound[a]

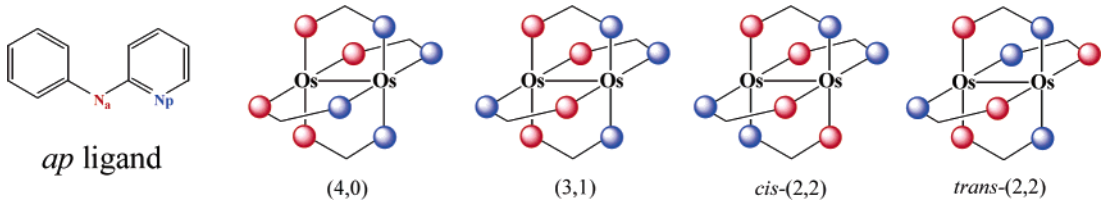

[a] N_a and N_p denote anilino and pyridino nitrogen centers, respectively.

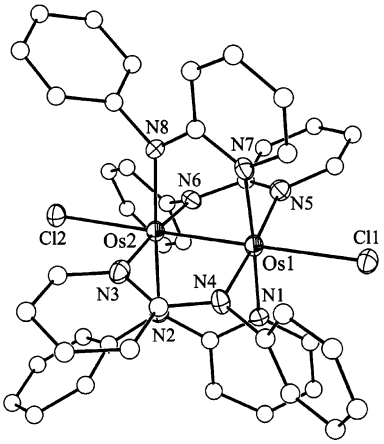

Figure 2. ORTEP plot of molecule **1b** at 30% probability level. Hydrogen atoms were omitted for clarity.

structure of **1a** on the most intense peaks (Figure S3 in the Supporting Information) and, hence, confirming the dominance of *cis*-(2,2) isomer in the bulk. On the other hand, the bulk sample prepared from hexanes/CH_2Cl_2 diffusion (conditions for **1b**) yielded a XPD pattern that is significantly different from the pattern calculated from **1b**. Hence, it is safe to conclude on the ground of XPD data that neither crystallization conditions afforded bulk sample of high isomeric purity.

Regioisomerism of $M_2(ap)_4$ type compounds stems from the inequivalency of two N-donor centers of the *ap* ligand: an anilino N (N_a) and a pyridino N (N_p). Among four possible regioisomers outlined in Chart 1, (4,0) and (3,1) compounds are polar while both *cis*- and *trans*-(2,2) are nonpolar. Clearly, the nonpolar *cis*-(2,2) compound was selectively deposited when the solution is highly polar (CH_3OH/CH_2Cl_2). Conversely, the polar (3,1) isomer was deposited when CH_3OH was replaced by hexanes. As noted earlier, $Os_2(ap)_4Cl_2$ became immobilized on both silica and alumina TLC plates, which prevents chromatographic identification and separation of isomers. The paramagnetism of $Os_2(ap)_4Cl_2$ excludes the utility of NMR technique in resolving the isomers. Consequently, the distribution of isomers in solution cannot be discerned presently and it is also unclear whether $Os_2(ap)_4Cl_2$ undergoes facile isomerization upon a change in solvent polarity. Similar regio-isomerism was also observed in both the Ru^{II}_2 and $Ru^{II}Ru^{III}$ compounds supported by 6-chloro-2-oxopyridinate, where the conversion of (4,0) isomer to (2,2) isomer was achieved under molten conditions (>150 °C).[2l]

Metric parameters determined for both compounds **1a**,**b** are collected in Table 1, and the two isomers have very similar bond lengths and angles around the Os_2 core. The

Table 1. Selected Bond Lengths (Å) and Angles (deg) for Compounds **1**

cis-(2,2) isomer, **1a**		(3,1) isomer, **1b**	
Os−Os′	2.3937(8)	Os(1)−Os(2)	2.3909(8)
Os−Cl	2.561(3)	Os(1)−Cl(1)	2.590(4)
Os−N(1)	2.064(9)	Os(2)−Cl(2)	2.512(4)
Os−N(2)	2.030(9)	Os(1)−N(1)	2.076(9)
Os−N(3)	2.079(9)	Os(1)−N(4)	2.028(8)
Os−N(4)	2.035(10)	Os(1)−N(5)	2.076(9)
		Os(1)−N(7)	2.064(9)
		Os(2)−N(3)	2.098(9)
		Os(2)−N(2)	2.044(9)
		Os(2)−N(6)	2.023(8)
		Os(2)−N(8)	2.031(9)
N(1)−Os−Os′	90.4(2)	N(1)−Os(1)−Os(2)	87.8(2)
N(2)−Os−Os′	88.2(2)	N(2)−Os(2)−Os(1)	88.8(2)
N(3)−Os−Os′	89.4(2)	N(5)−Os(1)−Os(2)	87.2(2)
N(4)−Os−Os′	88.2(2)	N(7)−Os(1)−Os(2)	89.4(2)
Os′−Os−Cl	176.75(7)	Os(2)−Os(1)−Cl(1)	177.72(7)
		N(3)−Os(2)−Os(1)	87.9(2)
		N(4)−Os(1)−Os(2)	89.4(2)
		N(6)−Os(2)−Os(1)	88.8(2)
		N(8)−Os(2)−Os(1)	87.4(2)
		Os(1)−Os(2)−Cl(2)	178.82(7)
N−Os−Os′−N′	5.3[5][a]	N−Os(1)−Os(2)−N′	13.4[5][a]

[a] Averaged twist angle; N and N′ centers belong to the same ap ligand.

Os−Os bond lengths, 2.3937(8) Å in **1a** and 2.3913(8) Å in **1b**, are identical within the experimental errors and comparable to those reported earlier for **1a** (2.3943(6) and 2.3976(5) Å).[15] The Os−Os distances found in other Os^{III}_2 compounds supported by N,N′-ligands are 2.379(2), 2.392(1), and 2.4672(6) Å for $Os_2(hpp)_4Cl_2$, $Os_2(ap)_3Cl_3$, and $Os_2(DtolF)_4Cl_2$, respectively.[12−14] The ranges of Os−N_a and Os−N_p bond lengths in compounds **1** are 2.025−2.038 and 2.064−2.081 Å, respectively, reflecting the stronger donor ability of anilino N center. The averaged axial Os−Cl bond length is about 2.55 Å and consistent with a weak Os−Cl bond. The unsymmetrical (3,1) isomer has a twist angle N−Os−Os′−N′ of 13.4°, which is significantly larger than that of the *cis*-(2,2) isomer (5.3°).

Synthesis and Structural Characterization of $Os_2(ap)_4(C_2Y)_2$. The aforementioned rapid degradation of $Os_2(ap)_4Cl_2$ on TLC plates is likely attributed to the lability of axial chloro ligand(s). Such lability became apparent in the synthesis of the phenylethynyl derivative: addition of LiC_2Ph to $Os_2(ap)_4Cl_2$ resulted in a dark red solution instantaneously and the complete conversion to the bis-adduct $Os_2(ap)_4(C_2Ph)_2$ (**2**) within 5 min. In comparison, alkynylation of $Ru_2(ap)_4Cl$ requires from 1 to 24 h.[7] Facile reactions between **1** and LiC_2Y similarly furnished $Os_2(ap)_4(C_2Y)_2$ with Y as Fc (**3**), $SiMe_3$ (**4**), and C_2SiMe_3 (**5**). It is clear from the most downfield region of the ^1H NMR spectrum of **2** recorded in $CDCl_3$ (Supporting Information) that there

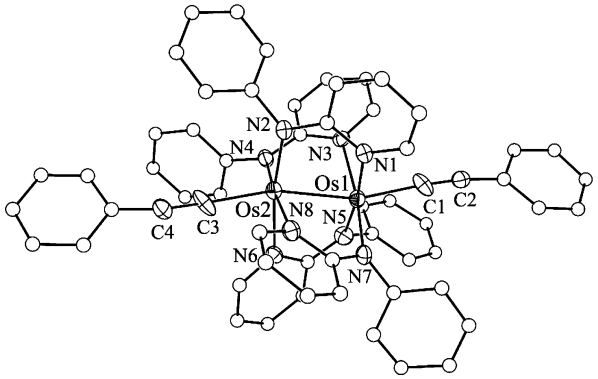

Figure 3. ORTEP plot of molecule **2a** at 30% probability level. Hydrogen atoms were omitted for clarity.

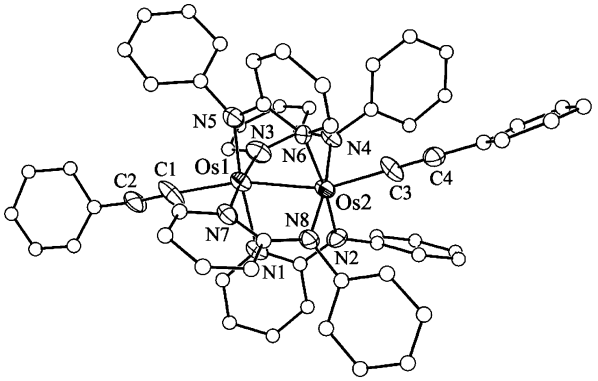

Figure 4. ORTEP plot of molecule **2b** at 30% probability level. Hydrogen atoms were omitted for clarity.

are two sets of signals attributed to py 6-H in ca. 95:5 ratio: three doublets in 2:1:1 ratio expected for the (3,1) isomer and a single doublet expected for the *cis*-(2,2) isomer. Similar distributions were also observed in the ^{1}H NMR spectra of compounds **3**−**5**. We were unable, however, to resolve the regioisomers chromatographically: each compound elutes as a single spot on TLC plate under a variety of solvent combinations spanning a large range of solvent polarity.

Similar to the parent compound **1**, compound **2** crystallizes as one of two regioisomers depending on conditions: the *cis*-(2,2) isomer (**2a**) from polar CH_3OH/CH_2Cl_2 solution and (3,1) isomer (**2b**) from weakly polar hexanes/THF solution. The (3,1) isomer of $Os_2(ap)_4(C_2SiMe_3)_2$ (**4b**) was also crystallized from hexanes/THF solution. Molecular structures of compounds **2a**,**b** and **4b** are shown in Figures 3−5, respectively, and their selected bond lengths and angles are gathered in Table 2. The Os−Os bond lengths are 2.4558(5), 2.4709(9), and 2.481(1) Å for compounds **2a**,**b** and **4b**, respectively, corresponding to lengthening of 0.06−0.08 Å from that of **1**. The elongation of the Os−Os bond is clearly attributed to the strong σ-donor nature of alkynyl ligands. The most distinguished feature of bis(alkynyl) species in comparison with the parent compound **1** is the severe structural distortion of the first coordination sphere around Os_2 core from an idealized D_{4h} symmetry. While the Os−N bond lengths are within 0.05 Å of each other in **1**, the variance in Os−N bond lengths is larger than 0.20 Å in each of **2a**,**b** and **4b**. Typically, each Os center has two shortened Os−N bonds that are trans to two elongated Os−N bonds.

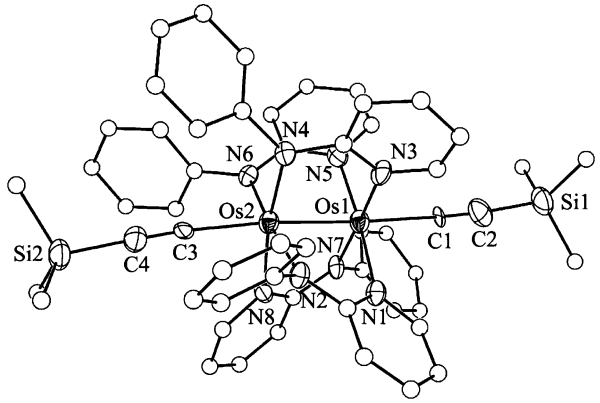

Figure 5. ORTEP plot of molecule **4b** at 30% probability level. Hydrogen atoms were omitted for clarity.

Table 2. Selected Bond Lengths (Å) and Angles (deg) of Compounds **2a**,**b** and **4b**

	2a	2b	4b
Os(1)−Os(2)	2.4558(5)	2.4709(9)	2.481(1)
Os(1)−C(1)	2.040(9)	2.13(2)	2.08(1)
Os(2)−C(3)	2.029(9)	1.97(1)	2.06(1)
Os(1)−N(1)	2.100(7)	2.17(1)	2.100(8)
Os(1)−N(3)	2.206(7)	2.04(1)	2.153(8)
Os(1)−N(5)	1.976(7)	2.130(9)	2.027(9)
Os(1)−N(7)	2.133(7)	2.11(1)	1.986(8)
Os(2)−N(2)	1.989(7)	1.98(1)	2.020(8)
Os(2)−N(4)	1.983(7)	2.12(1)	1.996(8)
Os(2)−N(6)	2.188(7)	1.99(1)	2.099(8)
Os(2)−N(8)	2.133(7)	1.984(9)	2.205(8)
C(1)−C(2)	1.20(1)	1.14(2)	1.10(2)
C(3)−C(4)	1.21(1)	1.24(2)	1.16(1)
Os(2)−Os(1)−C (1)	162.5(3)	165.6(4)	167.4(4)
Os(1)−Os(2)−C(3)	164.3(3)	159.1(4)	162.3(4)
N(1)−Os(1)−Os(2)	82.46(19)	79.6(3)	84.1(2)
N(3)−Os(1)−Os(2)	79.88(16)	93.1(4)	79.9(2)
N(5)−Os(1)−Os(2)	91.2(2)	80.6(3)	82.7(2)
N(7)−Os(1)−Os(2)	92.50(19)	82.6(3)	95.3(2)
N(2)−Os(2)−Os(1)	91.11(18)	94.0(3)	89.7(2)
N(4)−Os(2)−Os(1)	92.23(16)	82.2(3)	93.7(2)
N(6)−Os(2)−Os(1)	80.33(17)	92.6(3)	90.3(2)
N(8)−Os(2)−Os(1)	81.48(19)	91.0(3)	78.2(2)
N−Os(1)−Os(2)−N′[a]	23.2[3]	19.7[4]	19.45[3]

[a] Averaged twist angle; N and N′ centers belong to the same *ap* ligand.

While two crystallographically independent Os−C bond lengths are about the same in each of **2a** and **4b**, they differ by 0.15 Å in **2b**. The distortion is also evident in bond angles: the Os′−Os−C angles are deviated from linearity (180°) by at least 12° in all three structures, and variances in Os′−Os−N angles as large as 15° are also noted. The geometrical distortion found here closely tracks that observed earlier for bis(alkynyl) adducts of Ru^{III}_2 compounds,[7] which was attributed to a second-order Jahn−Teller effect.[9i]

The averaged C≡C bond length in **2a** is 1.20[1] Å, which does not appear to support a significant reduction in bond order as it does not deviate from the mean C≡C distance of 1.201(16) Å reported for $L_nM-C\equiv C-C/Si$.[16] This observation is consistent with the consensus that the d-π backbonding is insignificant in metal−σ-alkynyl compounds.[17]

(16) Manna, J.; John, K. D.; Hopkins, M. D. *Adv. Organomet. Chem.* **1995**, *38*, 79.
(17) (a) Lichtenberger, D. L.; Renshaw, S. K.; Wong, A.; Tagge, C. D. *Organometallics* **1993**, *12*, 3522. (b) Lichtenberger, D. L.; Renshaw, S. K.; Bullock, R. M. *J. Am. Chem. Soc.* **1993**, *115*, 3276.

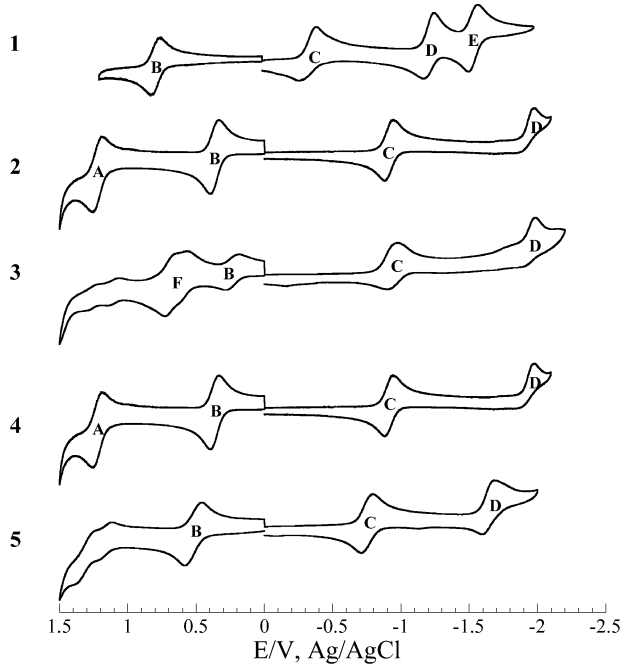

Figure 6. Cyclic voltammograms of compounds **1**−**5** recorded in 0.20 M THF solution of Bu_4NPF_6 at a scan rate of 0.10 V/s.

Substantial variances and deviations from the aforementioned norm of 1.201(16) Å are noted for C≡C bond lengths in compounds **2b** and **4b**, which are likely associated with the second-order J−T effect.

Electrochemical Studies of Compounds 1−5. Two Os_2-centered one-electron redox couples were reported for each of previously characterized Os^{III}_2 species supported by N,N′-bidentate bridging ligands, namely $Os_2(DtolF)_4Cl_2$ and $Os_2(hpp)_4Cl_2$.[12,13] The former exhibits an oxidation at 1.05 and a reduction at −0.15 V (versus Ag/AgCl), while the latter displays the first and second oxidations at 0.04 and 1.10 V, respectively. The contrast between $Os_2(DtolF)_4Cl_2$ and $Os_2(hpp)_4Cl_2$ reflects the extraordinary donor ability of *hpp* ligand, which preferentially stabilizes the higher oxidation states of dimetallic compounds.[18] As shown by the cyclic voltammogram (CV) in Figure 6, $Os_2(ap)_4Cl_2$ (**1**) is unique in exhibiting four one-electron couples. The most positive couple **B** is assigned as the Os_2 centered one-electron oxidation, and the remaining three couples **C**−**E** are one-electron reductions. While couples **B**, **D**, and **E** are (quasi)-reversible on the basis of their ΔE_p values, couple **C** is irreversible with a large ΔE_p value. The irreversibility is likely due to the loss of one Cl^- upon the reduction, as shown in Scheme 1, which is reminiscent of the established ECE process frequently observed for $Ru_2(DArF)_4Cl$ compounds.[3,9] The second reduction **D** is likely also Os_2 based and hence implicating the generation of an Os^{II}_2 species. The nature of the third reduction **E** remains uncertain presently. Assignment as $Os^{II}_2/Os^{II}Os^{I}$, though tempting, is unlikely considering that $Ru^{I}Ru^{II}$ has not yet been observed despite extensive studies of Ru_2 species supported by both *ap* and its derivatives. The one-electron oxidation couple $Os^{III}Os^{IV}/Os^{III}_2$ (**B**) is the only shared feature among three Os_2 compounds supported by different N,N′-bidentate ligands, and their potentials in ascending order are $hpp \ll ap < DtolF$, which clearly reflects the order of ligand donor ability ($hpp \gg ap > DtolF$).

The bis(alkynyl) derivatives **2**−**4** are also highly redox active and display at least three couples within the potential window accessible in THF, and their electrode potentials and spectroscopic data are collected in Table 3. The CV of $Os_2(ap)_4(C_2Ph)_2$ (**2**) consists of two reversible one-electron oxidations (**A** and **B**), one reversible reduction (**C**), and an irreversible reduction (**D**). As previously noted for $Os_2(hpp)_4Cl_2$, the appearance of the +2/+1 couple (**A**) in **2** is remarkable since its reversibility implies the presence of an Os^{IV}_2 species. Compared with the corresponding couples in **1**, both the reversible oxidation **B** and reduction **C** couples are cathodically shifted by 0.55 V. Both the observation of +2/+1 couple and large potential shift of **B** are the testament to the donor ability of phenylethynyl ligands in stabilizing high oxidation states. The strong donor ability of phenylethynyl ligands also resulted in a 0.68 V cathodic shift in **D**. The irreversibility of **D** is attributed to the fast dissociation of one of two phenylethynyl ligands upon the reduction. It is also interesting to compare the electrode potentials of **2** with that of its Ru analogue, namely $Ru_2(ap)_4(C_2Ph)_2$[8e] (also listed in Table 3): the first oxidation couple (**B**) of Os_2 is shifted cathodically by 0.39 V from that of Ru_2, and the first reduction couple (**C**) is similarly shifted by 0.48 V. These shifts are consistent with the fact that 5d metals are much electron-richer than their 4d congeners.

The CV of the (trimethylsilyl)ethynyl compound **4** has features almost identical with those of **2** and can be similarly assigned. In comparison, the corresponding couples of the (trimethylsilyl)butadiynyl compound **5** are anodically shifted due to the reduced donor ability of butadiynyl ligand: the couple **A** shifted out of potential limit permitted by THF (1.5 V), and couple **D** is 0.34 V more positive than that of **4** and quasireversible. The ferrocenylethynyl compound **3** displays Os_2-based couples at potentials comparable to those of **2** and **4** but with reduced reversibility. Ferrocenyl-based oxidations in **3** appear as a convoluted two-electron wave (**F**), a sharp contrast to the stepwise one-electron oxidations observed for *trans*-$Ru_2(DMBA)_4(C_2Fc)_2$.[9a] The sluggish redox behavior of **3** is likely due to the steric crowding caused by ferrocenyl groups, which results in ready decomposition of the molecule triggered by redox events.

Electronic Structures of Compounds 1-5. Compound **1** has a room-temperature effective moment (μ_{eff}) of 2.76 μ_B, consistent with a $S = 1$ ground state that may arise from either a $\sigma^2\pi^4\delta^2\pi^{*2}$ or $\sigma^2\pi^4\delta^2\delta^*\pi^*$ ground-state configuration. Previously, the former configuration was assigned to $Os_2(DtolF)_4Cl_2$ on the basis of the fitting of its $\chi-T$ curve with the zero-field-splitting model.[13] Due to the large zero-field-splitting constant ($D = 1350\ cm^{-1}$), the μ_{eff} of $Os_2(DtolF)_4Cl_2$ at room temperature is ca. 1.2 μ_B, which is much smaller than that of **1**. On the other hand, room-temperature μ_{eff} values around 2 μ_B have been observed for $Os_2(O_2CR)_4Cl_2$

(18) Cotton, F. A.; Gruhn, N. E.; Gu, J.; Huang, P.; Lichtenberger, D. L.; Murillo, C. A.; Dorn, L. O. V.; Wilkinson, C. C. *Science* **2002**, *298*, 1971.

Scheme 1. Electrochemical/Chemical Steps in $Os_2(ap)_4X_2$ (X = Cl and C_2Y)

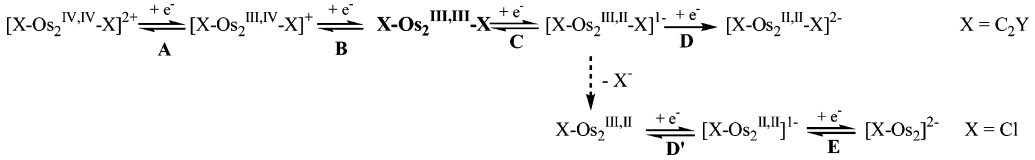

Table 3. Electrochemical and Spectroscopic Data for Compounds **1**−**5**[a]

param	**1**	**2**	**3**	**4**	**5**	$Ru_2(ap)_4(C_2Ph)_2$[d]
$E(+2/+1)$/V (ΔE_p/V, $i_{back}/i_{forward}$)	NA	1.19 (0.085, 0.98)	0.68 (0.134, 0.75)	1.23 (0.073, 0.77)	NA	NA
$E(+1/0)$/V (ΔE_p/V, $i_{back}/i_{forward}$)	0.78 (0.077, 0.91)	0.33 (0.071, 0.99)	0.24 (0.078, 0.67)	0.37 (0.051, 0.80)	0.52 (0.072, 0.93)	0.72
$E(0/-1)$/V (ΔE_p/V, $i_{back}/i_{forward}$)	−0.35 (0.132, 0.58)	−0.90 (0.071, 0.84)	−0.94 (0.097, 0.46)	−0.92 (0.065, 0.86)	−0.75 (0.077, 0.88)	−0.42
$E(-1/-2)$/V (ΔE_p/V, $i_{back}/i_{forward}$)	−1.24 (0.072, 0.43)	−1.92[b]	−1.99[b]	−1.98[b]	−1.64 (0.096, 0.88)	−1.58
$E(-2/-3)$/V (ΔE_p/V, $i_{back}/i_{forward}$)	−1.56 (0.070, 1.0)	NA	NA	NA	NA	NA
λ_{max}/nm (ϵ, $cm^{-1}\,M^{-1}$)	880 (4270)	781 (5090)	790 (sh)	800 (7200)	830 (sh)	1031 (3360)
	765 (sh)	487 (19 990)	464 (27 330)	615 (sh)	528 (8940)	629 (6930)
	630 (19 330)			483 (32 050)	478 (7580)	477 (5140)
	450 (11 600)					430 (5300)
$E(+1/0) - E(0/-1)$, V	1.13	1.23	1.18	1.29	1.27	1.14
E_{op},[c] eV	1.41	1.59	1.57	1.55	1.49	1.20

[a] Irreversible couple, E_{pa} is reported. [b] Irreversible couple, E_{pc} is reported. [c] $E_{op} = 10^7/(8065.5\lambda_{max})$, longest λ_{max} was used. [d] Data taken from ref 8e.

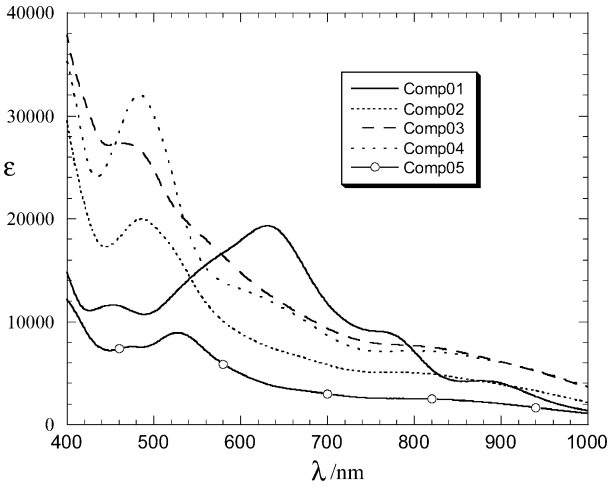

Figure 7. Visible−near infrared (vis−NIR) spectra of compounds **1**−**5** recorded in CH_2Cl_2.

type compounds,[19,20] and the $\chi-T$ characteristics of $Os_2(O_2CCMe_3)_4Cl_2$ are best described by the large zero-field-splitting of a ^3E_u state derived from the $\sigma^2\pi^4\delta^2\delta^*\pi^*$ configuration. In light of large μ_{eff} observed, a plausible ground-state configuration for **1** is $\sigma^2\pi^4\delta^2\delta^*\pi^*$, although the definitive answer awaits the measurement and analysis of its $\chi-T$ characteristics. Compound **1** also exhibits a complex vis-NIR absorption spectrum as shown in Figure 7, and peaks/shoulders at 630, 765, and 880 nm are *tentatively* assigned as σ(Cl) → σ^*(Os−Os), δ(Os−Os) → δ^*(Os−Os), and π^*(Os−Os) → δ^*(Os−Os) transitions, respectively, in analogy to the assignment for $Os_2(O_2CCMe_3)_4Cl_2$ by Miskowski and Gray.[20]

The diamagnetism, elongated Os−Os bond, and the signature second-order Jahn−Teller distortion observed for compounds **2**−**5** are convincing evidence of a $\pi^4\delta^2\pi^{*4}$ ground state configuration commonly found in $Ru_2(ap)_4(C_2Y)_2$ type compounds.[7] Finally, the vis-NIR spectra of compounds **2**−**5** (shown in Figure 7) consist of an intense peak around 500 nm and broad shoulders from 600 to 1000 nm. It is noteworthy that the spectra of $Os_2(ap)_4(C_2Y)_2$ are quite different from that of $Ru_2(ap)_4(C_2Y)_2$, which feature well-defined peaks at ca. 620 and 1030 nm.[7] We refrain from assigning the observed transitions in the absence of a reliable calculation.

Resonance Raman spectra of $Os_2(ap)_4Cl_2$ (**1**) and $Os_2(ap)_4(CCPh)_2$ (**2**) obtained with excitation into their electronic absorption bands exhibit several resonantly enhanced bands corresponding to vibrations associated predominantly with the equatorial ligands. Raman shifts and relative scattering intensities for the Raman spectra of **1** and **2** in THF solution obtained with 730 and 488 nm excitation, respectively, are set out in Table S1 (Supporting Information), and spectra are shown in Figure 8. For the most part, the Raman spectra of **1** and **2** exhibit a high degree of correlation with respect to band positions between 290 and 1700 cm^{-1}, indicating that the observed Raman bands correspond to vibrations that are largely localized on the equatorial *ap* ligands. Notably, the fact that the intensities of the bands belonging to the compounds (present in ∼10 mM concentration) are comparable to those belonging to the THF solvent (∼12 M as a neat liquid) in the spectra shown in Figure 8 indicates that the Raman bands of **1** and **2** are strongly enhanced, suggesting that there must be substantial distortions along *ap*-localized normal coordinates in the resonant excited states that are probed with these excitation wavelengths.

In addition to bands corresponding to *ap*-localized vibrations, the Raman spectrum of **2** obtained with 488 nm excitation exhibits a pair of reasonably intense, overlapping bands at 2078 and 2070 cm^{-1} that are attributed to the C−C stretching vibrations of the ethynyl groups. This assignment is supported by fact that these frequencies lie within the 2010−2190 cm^{-1} range defined by the ν(C−C) values reported for other metal complexes containing alkynyl ligands.[16] The fact that multiple C−C stretches were observed

(19) Cotton, F. A.; Ren, T.; Wagner, M. J. *Inorg. Chem.* **1993**, *32*, 965.
(20) Miskowski, V. M.; Gray, H. B. *Top. Curr. Chem.* **1997**, *191*, 41.

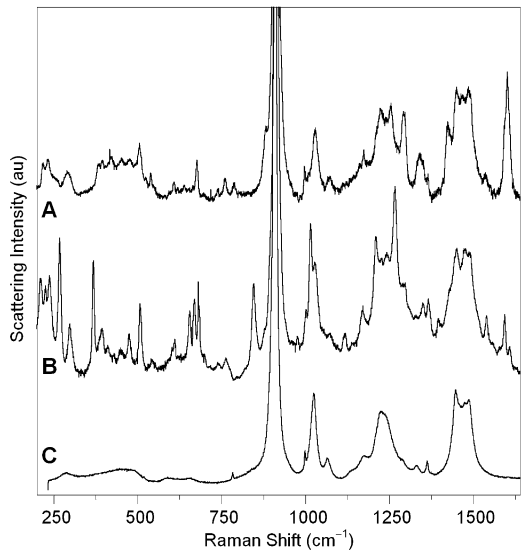

Figure 8. (A) Resonance Raman spectrum for a 10 mM solution of **2** in THF obtained with 488 nm excitation. (B) Resonance Raman spectrum for a 10 mM solution of **1** in THF obtained with 730 nm excitation. (C) Neat THF obtained with 488 nm excitation.

may be the result of the coexistence of the *cis*-(2,2) and (3,1) regioisomers in polar solvent (Chart 1).

The Raman spectra of **1** and **2** also exhibit several bands below 280 cm^{-1} that are likely candidates for ν(Os−Os). The range from 228 to 266 cm^{-1} has been previously established for ν(Os−Os) in vibrational studies of $Os_2(O_2CR)_4Cl_2$ compounds.[21] We should expect to observe the frequency of **1** within the 228−266 cm^{-1} region as it possesses an Os−Os triple bond, whereas **2** possess only an Os−Os single bond. Our expectation was that a band associated with the Os≡Os stretch of **1** would be significantly shifted to lower energy in the spectrum of **2** given the reduction in bond order. Unfortunately, each of the low-frequency bands identified in the spectra of **2** is slightly shifted from its position in the corresponding spectra of **1**, rendering it impossible to unambiguously assign one of them to ν(Os−Os). This observation is unsurprising, though, given the fact that extensive vibrational studies of the complexes $Mo_2(PMe_3)_4Cl_4$ and $[NBu^n_4]_4[Mo_2(CN)_8]\cdot 8CHCl_3$ reveal that the Mo−Mo oscillator couples strongly to vibrations involving metal−ligand coordinates.[22] It is likely that the Os−Os oscillator is similarly coupled to metal−ligand (and possibly ligand-localized) vibrations for the compounds under study herein and that two or more bands in the Raman-shift region below 280 cm^{-1} have ν(Os−Os) character.

Conclusion

Synthesis of both $Os_2(ap)_4Cl_2$ and the novel alkynyl derivatives $Os_2(ap)_4(C_2Y)_2$ and their characterization are presented in this contribution. The rich electrochemical and spectroscopic properties exhibited by these compounds make them alluring candidates for future theoretical studies, which can be challenging due to various complications associated with 5d metals. The observation of a reversible +2/+1 couple for compound **2** implies the feasibility of isolating an Os^{IV}_2 species based on a bis(alkynyl) derivative—a potentially rewarding endeavor currently pursued in our laboratory.

Experimental Section

Phenylacetylene and *n*-butylithium (1.6 M in hexane) were purchased from Aldrich. $Os_2(OAc)_4Cl_2$,[23] 2-anilinopyrdine,[3] and ferrocenylacetylene[24] were prepared according to literature procedures. Syntheses were performed in a dry argon atmosphere using standard Schlenk-line techniques. ^{1}H NMR spectra were recorded on a Bruker AVANCE300 NMR spectrometer with chemical shifts (δ) referenced to the residual $CHCl_3$. Infrared spectra were recorded on a Perkin-Elmer 2000 FT-IR spectrometer using KBr disks. Vis-NIR spectra in CH_2Cl_2 were obtained with a Perkin-Elmer Lambda-900 UV−vis spectrophotometer. Magnetic susceptibilities were measured at 294 K with a Johnson Matthey Mark-I magnetic susceptibility balance. Cyclic voltammograms were recorded in 0.2 M $(n\text{-Bu})_4NPF_6$ solution (CH_2Cl_2, N_2-degassed) on a CHI620A voltammetric analyzer with a glassy carbon working electrode (diameter = 2 mm), a Pt-wire auxiliary electrode, and a Ag/AgCl reference electrode. The concentration of diosmium species is always 1.0 mM. The ferrocenium/ferrocene couple was observed at 0.60 V (vs Ag/AgCl) at the experimental conditions. Due to the expensive nature of Os-containing reagents, none of compounds reported herein were submitted for combustion analysis.

Synthesis of $Os_2(ap)_4Cl_2$ (1). To a 100 mL round-bottom flask was charged $Os_2(OAc)_4Cl_2$ (0.443 g, 0.64 mmol), 2-anilinopyridine (0.878 g, 5.16 mmol), and 40 mL of toluene, to which a micro Soxhlet extractor with a glass thimble containing a 1:1 mixture of K_2CO_3 and sand was mounted. The mixture was gently refluxed under ambient atmosphere for 3 days and then cooled and filtered. After the removal of toluene via distillation and excess H*ap* via sublimation, the residue was recrystallized from 30 mL of hot CH_3OH to yield 0.49 g of blue crystalline materials (67% based on Os). Data for **1**: MS-FAB (*m*/*e*, based on ^{190}Os) 1129 [MH$^+$]; molar susceptibility (χ_{mol}) 3.23 × 10^{-3} emu, μ_{eff} = 2.76 μ_B.

Synthesis of $Os_2(ap)_4(C_2Ph)_2$ (2). To a 20 mL THF solution of phenylacetylene (0.53 mmol) at −78 °C was added 0.34 mL of 1.6 M n-BuLi. The mixture was allowed to warm to room temperature to yield an off-white slurry, which was transferred to a 40 mL THF solution of $Os_2(ap)_4Cl_2$ (0.100 g, 0.088 mmol). The reaction mixture was stirred at room temperature and became a clear dark red solution in 5 min. TLC analysis (hexanes:triethylamine:ethyl acetate = 10:1:1) revealed the formation of a single product (R_f = 0.32) and the complete consumption of $Os_2(ap)_4Cl_2$. After the solvent removal, the residue was purified by column chromatography using silica gel which was deactivated by triethylamine to yield **2** as dark red solid (0.112 g, 80%). Data for **2**: ^{1}H NMR ($CDCl_3$) for (3,1) isomer, 10.34 (d, 2H, 6-py), 10.18 (d, 1H, 6-py), 9.68 (d, 1H, 6-py), 7.85−7.76 (m, 4H, aromatic), 7.44−7.24 (m, 8H, aromatic), 7.06−6.81 (m, 12H, aromatic), 6.65−6.37 (m, 10H, aromatic), 5.97 (m, 3H, aromatic), 5.89 (d, 1H, aromatic), 5.28 (t, 1H, aromatic), 5.06 (t, 1H, aromatic), 4.89 (t, 2H, aromatic), for (2,2)-isomer, 9.80 (d, 6-py); MS-FAB (*m*/*e*, based on ^{190}Os) 1261 [MH$^+$]; IR ν(C≡C)/cm^{-1} 2064 (m).

(21) (a) Clark, R. J. H.; Hempleman, A. J.; Tocher, D. A. *J. Am. Chem. Soc.* **1988**, *110*, 5968. (b) Clark, R. J. H.; Hempleman, A. J. *J. Chem. Soc., Dalton Trans.* **1988**, 2601.

(22) (a) Clark, R. J. H.; Firth, S.; Sella, A.; Miskowski, V. M.; Hopkins, M. D. *J. Chem. Soc., Dalton Trans.* **2000**, 2928. (b) John, K. D.; Miskowski, V. M.; Vance, M. A.; Dallinger, R. F.; Wang, L. C.; Geib, S. J.; Hopkins, M. D. *Inorg. Chem.* **1998**, *37*, 6858.

(23) Behling, T.; Wilkinson, G.; Stephenson, T. A.; Tocher, D. A.; Walkinshaw, M. D. *J. Chem. Soc., Dalton Trans.* **1983**, 2109.

(24) Doisneau, G.; Balavoine, G.; Fillebeen-Khan, T. *J. Organomet. Chem.* **1992**, *425*, 113.

Table 4. Crystal Data for Compounds **1a**,**b**, **2a**,**b**, and **4b**

param	**1a**·2MeOH	**1b**·2H_2O	**2a**	**2b**·H_2O	**4b**
chem formula	$C_{46}H_{44}Cl_2N_8O_2Os_2$	$C_{44}H_{40}Cl_2N_8O_2Os_2$	$C_{60}H_{46}N_8Os_2$	$C_{60}H_{48}ON_8Os_2$	$C_{54}H_{54}N_8Os_2Si_2$
fw	1192.2	1164.1	1259.5	1277.5	1251.63
space group	*Pbca* (No. 61)	$P2_1/n$ (No. 14)	$P2_12_12_1$ (No. 19)	$P\bar{1}$ (No. 2)	$P\bar{1}$ (No. 2)
a, Å	14.8766(15)	17.3208(15)	14.5896(16)	12.302(2)	10.745(5)
b, Å	16.2444(17)	13.1381(11)	16.7490(15)	14.129(2)	15.977(8)
c, Å	17.6895(15)	19.2668(16)	20.599(3)	18.044(4)	17.931(9)
α, deg				109.901(16)	70.64(3)
β, deg		93.637(2)		99.449(19)	87.14(6)
γ, deg				103.367(13)	78.87(4)
V, Å^3	4274.9(7)	4375.6(6)	5033.6(9)	2766.2(9)	2849(2)
Z	4	4	4	2	2
T, °C	27	27	27	27	27
λ(Mo Kα), Å	0.710 73	0.710 73	0.710 73	0.710 73	0.710 73
ρ_{calc}, g cm^{-3}	1.849	1.767	1.662	1.512	1.459
μ, mm^{-1}	6.113	5.970	5.092	4.633	4.537
R1	0.027	0.047	0.046	0.058	0.047
wR2	0.069	0.131	0.075	0.149	0.110

Synthesis of $Os_2(ap)_4(C_2Fc)_2$ (3). Reaction between **1** and lithiated ferrocenylacetylene under conditions the same as that of **2** yielded compound **3** as dark red solid in 70% yield. Data for **3**: R_f 0.36; ^{1}H NMR ($CDCl_3$) for (3,1) isomer, 10.20 (d, 2H, 6-py), 9.78 (d, 1H, 6-py), 9.42 (d, 1H, 6-py), 7.40−7.65 (m, 4H, aromatic), 7.10−7.38 (m, 8H, aromatic), 6.80−7.10 (m, 5H, aromatic), 6.63 (d, 2H, aromatic), 6.20 (d, 2H, aromatic), 5.99 (d, 2H, aromatic), 5.82 (d, 2H, aromatic), 5.50 (d, 2H, aromatic), 5.15−5.43 (m, 2H, aromatic), 5.00 (t, 1H, aromatic), 4.66 (t, 2H, aromatic) 4.24 (s, 5H, Cp), 4.40 (s, 2H, Cp), 4.35 (s, 2H, Cp), 4.09 (s, 5H, Cp), 3.97 (s, 2H, Cp), 3.54 (s, 2H, Cp), for (2,2)-isomer, 9.22 (d, 6-py); MS-FAB (*m*/*e*, based on ^{190}Os) 1476 [MH$^+$]; IR ν(C≡C)/cm^{-1} 2010 (m).

Synthesis of $Os_2(ap)_4(C_2TMS)_2$ (4). Reaction between **1** and 4 equiv of LiC_2SiMe_3 under conditions the same as that of **2** resulted in compound **4** as dark brown solid in 76% yield. Data for **4**: R_f 0.67; ^{1}H NMR ($CDCl_3$) for (3,1) isomer, 9.85 (d, 2H, 6-py), 9.67 (d, 1H, 6-py), 9.20 (d, 1H, 6-py), 7.35−6.80 (m, 16H, aromatic), 6.68−6.26 (m, 6H, aromatic), 6.18−5.82 (m, 4H, aromatic), 5.78−5.22 (m, 6H,) 0.36 (s, 9H, CH_3), 0.01(s, 9H, CH_3), for (2,2)-isomer, 9.42 (d, 6-py); MS-FAB (*m*/*e*, based on ^{190}Os) 1253 [MH$^+$]; IR ν(C≡C)/cm^{-1} 1995 (s), 2010 (s).

Synthesis of $Os_2(ap)_4(C_4TMS)_2$ (5). Reaction between **1** and 2 equiv of LiC_4SiMe_3 under conditions the same as that of **2** resulted in compound **5** as dark red solid in 74% yield. Data for **5**: R_f 0.53; ^{1}H NMR ($CDCl_3$) for (3,1) isomer, 9.47 (d, 2H, 6-py), 9.06 (d, 1H, 6-py), 8.87 (d, 1H, 6-py), 7.38−6.82 (m, 16 H, aromatic), 6.62−5.25 (m, 16 H, aromatic), 0.33 (s, 9H, CH_3), 0.08 (s, 9H, CH_3), for (2,2)-isomer, 9.06 (d, 6-py), 0.30 (s, CH_3), 0.25 (s, CH_3); MS-FAB (*m*/*e*, based on ^{190}Os) 1301 [MH$^+$]; IR ν(C≡C)/cm^{-1} 2100 (s), 2160 (s).

Resonance Raman Spectroscopy. All manipulations were carried out under a dry nitrogen atmosphere using standard drybox techniques. Tetrahydrofuran (THF) was deoxygenated by distillation from sodium benzophenone ketyl under nitrogen prior to use. Resonance Raman spectra for samples in THF solution sealed in NMR tubes were obtained using 488 nm excitation from a Spectra Physics 2045 Ar-ion laser and 730 nm excitation from an Ar-ion-pumped Spectra Physics 3900 Ti:sapphire laser. Scattered light was collected and directed into a commercial spectrometer operated as either a single-stage or a triple-stage spectrograph equipped with an 1800 grooves/mm grating in the final stage; use of the single-stage spectrograph requires that the scattered light first be passed through a holographic notch filter (Kaiser) to reduce contributions from Rayleigh scattering. Scattering intensities were recorded using a liquid-nitrogen-cooled CCD detector (Princeton Instruments). A polarization scrambler was placed at the entrance slit of the spectrograph to minimize distortions in the observed scattering intensities due to wavelength-dependent response of the spectrograph to polarized light. Typical excitation powers and integration times were 20−40 mW (at the sample) and 30−120 min, respectively. Raman shifts were calibrated using either an external reference of 4-acetamidophenol[25] (Tylenol) or the emission lines from low-intensity Ne and Ar lamps. The dispersion characteristics of our instrumentation typically require the acquisition and concatenation of several spectral windows to encompass the Raman shift range from ca. 150−2200 cm^{-1}. Adjacent spectral windows containing sufficient overlap of bands permit accurate representation of relative intensities (uncorrected for instrument response).

X-ray Data Collection, Processing, and Structure Analysis and Refinement. Single crystals were grown via either slow diffusion of methanol into a CH_2Cl_2 solution (**1a** and **2a**), or slow diffusion of hexanes into a CH_2Cl_2 solution (**1b**), or slow evaporation of a THF/hexanes solution (**2b** and **4b**). The X-ray intensity data were measured at 300 K on a Bruker SMART1000 CCD-based X-ray diffractometer system using Mo Kα (λ = 0.710 73 Å). Thin plates of dimension 0.20 × 0.08 × 0.06 mm^3 (**1a**), 0.15 × 0.14 × 0.06 mm^3 (**1b**), 0.22 × 0.10 × 0.07 mm^3 (**2a**), 0.25 × 0.20 × 0.02 mm^3 (**2b**), and 0.36 × 0.15 × 0.04 mm^3 (**4b**) were cemented onto a quartz fiber with epoxy glue for data collection. Data were measured using ω scans of 0.3°/frame such that a hemisphere (1271 frames) was collected. No decay was indicated for any of five data sets by the recollection of the first 50 frames at the end of each data collection. The frames were integrated with the Bruker SAINT software package[26] using a narrow-frame integration algorithm, which also corrects for the Lorentz and polarization effects. Absorption corrections were applied using SADABS supplied by George Sheldrick. Powder X-ray diffraction measurements of compounds **1a**,**b** were performed on approximately 30 mg of crushed single crystals suspended in a vacuum grease using a Philips MRD diffractometer operating with Cu Kα radiation (1.540 56 Å) at 2.2 kW.

The single-crystal structures were solved and refined using the Bruker SHELXTL (version 5.1) software package[27] in the space groups *Pbca*, $P2_1/n$, $P2_12_12_1$, $P\bar{1}$, and $P\bar{1}$ for crystals **1a**,**b**, **2a**,**b**, and **4b**, respectively. Positions of all non-hydrogen atoms of diosmium moieties were revealed by the direct method. The asymmetric unit of **1a** contains half of the molecule, while those

(25) Raman shifts for 4-acetamidophenol can be found at http://www.chemistry.ohio-state.edu/~rmccreer/freqcorr/images/tylenol.html.

(26) *SAINT V 6.035 Software for the CCD Detector System*; Bruker-AXS Inc.: Madison, WI, 1999.

of **1b**, **2a**,**b**, and **4b** all contain one independent molecule. With all non-hydrogen atoms being anisotropic and all hydrogen atoms in calculated position and riding mode the structure was refined to convergence by least-squares method on F^2, SHELXL-93, incorporated in SHELXTL.PC V 5.03. Relevant information on the data collection and the figures of merit of final refinement are listed in Table 4.

Acknowledgment. We thank the generous support from the National Science Foundation (Grant CHE 0242623 to T.R.), the University of Miami (CCD diffractometer fund), and the Los Alamos National Laboratory's Laboratory Directed Research and Development program (to K.D.J.). R.E.D.R. was a G. T. Seaborg Institute for Transactinium Science Postdoctoral Fellow.

(27) (a) *SHELXTL 5.03 (WINDOW-NT Version), Program library for Structure Solution and Molecular Graphics*; Bruker-AXS Inc.: Madison, WI, 1998. (b) Sheldrick, G. M. *SHELXS-90, Program for the Solution of Crystal Structures*; University of Göttigen: Göttigen, Germany, 1990. (c) Sheldrick, G. M., *SHELXL-93, Program for the Refinement of Crystal Structures*; University of Göttigen: Göttigen, Germany, 1993.

Supporting Information Available: Text giving details of the ^{1}H NMR spectra of compound **2**, XPD data for compounds **1a**,**b**, the list of vibrational frequencies and Raman scattering intensities for **1** and **2**, and X-ray crystallographic files in CIF format for the structure determinations of compounds **1a**,**b**, **2a**,**b**, and **4b**. This material is available free of charge via the Internet at http://pubs.acs.org.

IC050496R